THE JOURNAL OF PHYSICAL CHEMISTRY B

pubs.acs.org/JPCB

Article

Computational NMR Study of Ion Pairing of 1-Decyl-3-methyl-imidazolium Chloride in Molecular Solvents

Dovilė Lengvinaitė, Vytautas Klimavičius, Vytautas Balevicius, and Kęstutis Aidas*

Cite This: *J. Phys. Chem. B* 2020, 124, 10776–10786

Read Online

ACCESS | Metrics & More | Article Recommendations

ABSTRACT: The ^{1}H NMR spectra of 10^{-5} mole fraction solutions of 1-decyl-3-methyl-imidazolium chloride ionic liquid in water, acetonitrile, and dichloromethane have been measured. The chemical shift of the proton at position 2 in the imidazolium ring of 1-decyl-3-methyl-imidazolium (H2) is rather different for all three samples, reflecting the shifting equilibrium between the contact pairs and free fully solvated ions. Classical molecular dynamics simulations of the 1-decyl-3-methyl-imidazolium chloride contact ion pair as well as of free ions in water, acetonitrile, and dichloromethane have been conducted, and the quantum mechanics/molecular mechanics methods have been applied to predict NMR chemical shifts for the H2 proton. The chemical shift of the H2 proton was found to be primarily modulated by hydrogen bonding with the chloride anion, while the influence of the solvents—though differing in polarity and capabilities for hydrogen bonding—is less important. By comparing experimental and computational results, we deduce that complete disruption of the ionic liquid into free ions takes place in an aqueous solution. Around 23% of contact ion pairs were found to persist in acetonitrile. Ion-pair breaking into free ions was predicted not to occur in dichloromethane.

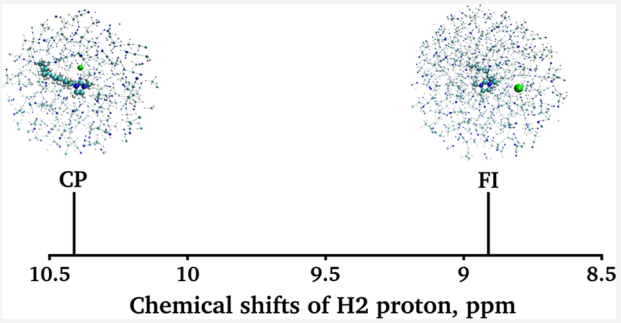

INTRODUCTION

Ionic liquids (ILs) are salts with a melting point below 100 °C. Because ILs are typically composed of asymmetric organic cations and organic or inorganic anions, many of them remain liquid at or near room temperature.[1−4] ILs are generally regarded as being environmentally friendly solvents because they are nonvolatile, thermally stable, and recyclable. Many of their chemical and physical properties, such as acidity, electrical conductivity, ability to solvate solutes of different polarities, or miscibility with water as well as with organic solvents, can in principle be tailored for specific needs due to the seemingly unlimited flexibility in choosing the cationic and anionic species. A few areas of applications of these task-specific ILs include cellulose processing,[5] lubrication,[6] solvent-free electrolytes for solar cells,[7] CO_2 capture,[8,9] or extraction of metals from aqueous solutions.[10,11] Furthermore, ILs have demonstrated their potential in separation technologies,[12−14] organic syntheses and catalyses,[15−20] and electrochemical devices.[21−23]

Pure ILs are, however, seldom dealt with. Many of them are very hygroscopic and may readily absorb considerable amounts of water from the atmosphere.[24] Water may have both detrimental and favorable effects on the properties of ILs. For example, even trace amounts of water were seen to significantly diminish the solubility of cellulose in the 1-butyl-3-methyl-imidazolium chloride, [C4mim][Cl], IL.[5] On the other hand, the role of water was recognized as crucial for the stabilization of the native state of the cytochrome *c* protein in the biocompatible IL over periods of time significantly exceeding those seen in protein's natural aqueous environment.[25,26] Mixtures of IL and water may also exhibit unexpected behavior such as recently demonstrated increasing viscosity induced by heating the sample.[27] ILs are notoriously viscous, and the addition of a molecular cosolvent reduces the viscosity considerably and thus renders these liquids easier to handle.[28,29] The conductivities of pure ILs are typically rather low, but they are markedly higher for their mixtures with traditional solvents.[30] Mixtures of IL and acetonitrile were seen to possess an improved electrochemical window as compared to those of pure components,[31] and they have been used as electrolytes in electrochemical production of graphene[32] or for the electrocatalytic enhancement of the reduction of CO_2 to CO.[33]

To rationalize the modulating effect of the molecular solvent on the properties of the IL, a thorough understanding of intermolecular interactions between the constituent ionic and

Received: August 14, 2020
Revised: October 9, 2020
Published: November 12, 2020

https://dx.doi.org/10.1021/acs.jpcb.0c07450
J. Phys. Chem. B 2020, 124, 10776−10786

molecular species that govern molecular association in the mixture is crucial.[3,4] At lower concentrations of the IL in the molecular solvent, ion pairing is an important phenomenon, where the dynamic equilibrium between free ions, solvent-separated and contact ion pairs, and higher-order neutral or charged ionic aggregates is established, which is sensitive to the concentration of the IL.[34,35] There is a general trend for polar solvents to be capable of breaking the ion pairs into separate ions, while nonpolar solvents tend to favor ion aggregation.[34,36] This can be exemplified by the association constants of 1-butyl-3-methyl-imidazolium tetrafluoroborate, [C4mim][BF_4], which range from the order of 10^5 dm^3/mol in dichloromethane, DCM, to 10^{-1} dm^3/mol in water.[35] Indeed, the low-concentration aqueous solutions of ILs behave as traditional electrolytes, where ions are virtually completely solvated,[35,37−41] although in some instances ion pairing was detected even at rather low concentrations of the IL.[42,43] Dimethyl sulfoxide, DMSO, has also demonstrated the capability of breaking ionic aggregates into separate ions,[41,44−46] but, here too, some ILs have displayed slight association at high dilutions.[35,47] Remarkably, however, higher-order supramolecular ionic clusters were found to persist at rather low concentrations of [C4mim][Cl] IL in DMSO.[37] Even though acetonitrile is rather similar to DMSO in polarity, it does not seem to break ionic aggregates into separate ions, apparently due to the poorer hydrogen-bond accepting abilities.[45,48−50] Varying degrees of dissociation of the [C4mim]-based[35,51,52] and ammonium-based[41] ILs in acetonitrile solution were, however, reported. At low concentrations in nonpolar solvents, ILs tend to form supramolecular aggregates,[35,44,51,53−55] although lone contact ion pairs were seen to be the dominant association pattern for some ILs in chloroform[47] and dichloromethane.[56,57] However, the dissociation of [C4mim][Cl] ion pairs into separate ions in solutions of chloroform and carbon tetrachloride has been observed very recently.[58,59]

Nuclear magnetic resonance, NMR, spectroscopy has proven to be a useful tool in structural and dynamical investigations of IL systems.[3,4,60−62] For the imidazolium family of ILs, the chemical shift of the H2 proton has been recognized to be a sensitive probe of the local environment of the imidazolium cation[37,50,52,53,55,63] because the C2−H2 bond is the most acidic bond in the imidazolium ring and thus is typically the most favorable site for hydrogen bonding.[64,65] In one particular case, the NMR signal of the H2 proton in the solutions of [C10mim][Br] IL has displayed a rather strong solvent dependence as it was found to be the highest at about 10.6 ppm in dichloromethane, DCM, and the lowest at about 8.9 ppm in water with an intermediate chemical shift at around 10.3 ppm recorded in acetonitrile, ACN, all w.r.t. $Si(CH_3)_4$.[66] These results clearly reflect the shifting equilibrium between ionic aggregates and free ions in these three solvents, which differ in both polarity and capability for hydrogen bonding. To elucidate the effect of different molecular solvents on ion pairing at low concentrations of the IL, we have performed the ^{1}H NMR measurements of 1-decyl-3-methyl-imidazolium chloride, [C10mim][Cl], in solutions of water, ACN, and DCM, where the molar fraction of the IL was as low as 10^{-5}. The concentration of the IL in all three solvents was held as low as possible so that we may rely on the assumption that the equilibrium is mainly established between contact ion pairs and free ions, thus hopefully excluding the possibility of higher-order ionic aggregates.

To provide valid rationalizations of experimental results, the NMR shielding constants of the C10mim cation in the ion pair and in its free solvated state are necessary yet virtually unachievable by measurements due to the fast chemical exchange. To assess the equilibrium between different states of the ions and to get a detailed microscopic picture of the ion pairing phenomenon in the studied mixtures of IL and three molecular solvents, we rely on an integrated computational approach. This approach incorporates classical molecular dynamics, MD, simulations for sampling the phase space of the molecular system at given thermodynamic conditions and the combined quantum mechanics/molecular mechanics, QM/MM, model for calculations of the NMR shielding constants.[67,68] Such computational scheme allows accounting for the solvent effects on the NMR properties in an effective and accurate manner,[69−76] and it was demonstrated to be essential for qualitatively correct predictions of NMR spectra of IL systems as well.[77,78]

METHODS

Classical MD Simulations. Classical MD simulations were performed to address structural features of the [C10mim][Cl] contact ion pair in the solutions of water, ACN, and DCM as well as to generate a number of statistically uncorrelated molecular configurations to be used in the subsequent QM/MM calculations of the electronic NMR properties. All MD simulations have been conducted using the Amber12 program.[79] The geometries of the C10mim cation in all-anti conformation of the decyl group, of the ACN, and of the DCM molecules were optimized at the HF/6-31G* level of theory[80,81] using the Gaussian09 program.[82] We have employed Lennard−Jones parameters for the C10mim cation as well as for the chloride anion taken from ref 83, where the parameters based on the Amber force field were developed specifically for the imidazolium family of ILs. For ACN and DCM, parameters from the general Amber force field[84,85] were employed. The point charges for C10mim, ACN, and DCM molecules were derived by means of the restrained electrostatic potential, RESP, procedure[86] as implemented in the Antechamber module[87] of Amber12. These point charges were based on the electrostatic potentials computed at the HF/6-31+G* level using the Gaussian09 program, in accordance with the procedure used in ref 83. The standard TIP3P potential was used for water molecules.[88] The solutions of [C10mim][Cl] in DCM, ACN, and water were represented by one [C10mim][Cl] ion pair and 2030 DCM, 2490 ACN, and 2735 water molecules, respectively. In addition, we have performed MD simulations using two different initial conditions in each of the three cases—starting from the contact ion pair or from the configuration where both ions are free and completely solvated by the solvent. The initial configurations were constructed using the Packmol program.[89]

MD simulations were carried out using the Sander module of Amber12. Periodic boundary conditions were employed, and a cutoff of 10 Å was used for nonbonded interactions. The SHAKE algorithm[90] was imposed to constrain all bonds involving hydrogen atoms, and the SETTLE scheme[91] was used to ensure rigidity of the water molecules in the simulations. The equations of motion were integrated using the leap-frog algorithm with a time step of 1 fs. The temperature was set to 297.15 K in all simulations and controlled using the Langevin thermostat with a collision frequency of 3.0 ps^{-1}. For each of the simulated systems, an

https://dx.doi.org/10.1021/acs.jpcb.0c07450
J. Phys. Chem. B 2020, 124, 10776−10786

initial simulation in the NPT ensemble at the pressure set to 1 bar was conducted for 300 ps to equilibrate the density. We then switched to the NVT ensemble, equilibrated the system for another 200 ps, and finally continued with the production run of 1 ns. Statistical equilibrium was assessed by monitoring the convergence of the thermodynamic properties. Molecular configurations were recorded every 0.5 ps for further analysis.

Electronic Structure Calculations. To select a reliable electronic structure method for the calculation of the NMR isotropic shielding constants, we have performed a series of benchmark calculations on a 1,3-dimethylimidazolium, C1mim, cation. The C_{2v} geometry of the isolated C1mim cation was optimized by the B3LYP functional[92] together with the aug-cc-pVTZ basis set[93,94] using the Gaussian09 program. The B3LYP,[92] PBE0,[95] and KT3[96] density functionals as well as the *ab initio* MP2 method were considered. The coupled cluster singles and doubles, CCSD, computations were performed to gauge the accuracy of the aforementioned methods. Basis sets due to Ahlrichs[97] (def2-X(Z)VP(D), where X = S, T, Q) and Dunning[93,94,98] (aug-cc-p(C)VXZ, where X = D, T, Q) were considered. The gauge-including atomic orbital, GIAO, approach was used to obtain origin-independent NMR isotropic shielding constants. The density functional theory, DFT, calculations were performed using the Gaussian09 program,[99] while MP2 and CCSD computations were done using CFOUR.[100]

The QM/MM method based on the GIAO-DFT approach[68,101] implemented in the Dalton electronic structure program[99] has been used for the calculations of NMR isotropic shielding constants. The point charges for ACN and DCM molecules used in the QM/MM calculations were derived by fitting to the electrostatic potential computed at the B3LYP/aug-cc-pVTZ method along with the polarizable continuum method, PCM,[102] according to the CHELPG procedure together with the constraint on the magnitude of the dipole moment.[103] These calculations were conducted using the Gaussian09 program. For water molecules, point charges from the TIP3P force field[88] were used, and we have also employed the polarizable potential due to Ahlström[104] for comparative purposes. The liquid-state results for NMR shielding constants are obtained as statistical averages over 100 molecular configurations selected from the MD trajectories at regular intervals of 10 ps. We have applied a spherical cutoff radius centered at the center of mass of the C10mim cation for every molecular configuration, resulting in an average number of 1050 water and DCM or 1290 ACN solvent molecules included in a single QM/MM calculation.

We have also employed the so-called supermolecular approach to account for solvent effects on the NMR properties of the C10mim cation. Here, the geometries of the C10mim cation and its aggregates with chloride anion as well as with water, ACN, and DCM molecules were optimized using the B3LYP functional along with the 6-31++G** basis set.[81] The Gaussian09 program was employed to carry out these geometry optimizations and calculations of NMR properties using the PCM model with default settings for all solvents of water, ACN, and DCM.

Experimental ^{1}H NMR Measurements. The [C10mim][Cl] IL from Ionic Liquids Technologies GmbH was dried under vacuum at 333 K for 24 h. Samples were prepared directly in 5 mm NMR tubes using a micropipette and in parallel weighing the samples to ensure exact concentration. A capillary insert filled with the mixture of D_2O and sodium trimethylsilylpropanesulfonate, DSS, was used for lock and ^{1}H NMR chemical shift referencing (δ = 0 ppm). The chemical shifts were subsequently referenced against tetramethylsilane, TMS, taking δ(TMS) = 0.02 ppm. NMR measurements were carried out on a Bruker AVANCE III HD 400 MHz NMR spectrometer using a BBO high-resolution probe. The sample temperature was set to 298 ± 0.5 K. For ^{1}H NMR spectra, 4096−8192 scans were accumulated using 5 s of recycling delay.

RESULTS AND DISCUSSION

Method Analysis. To select an appropriate electronic structure method for the computation of the ^{1}H NMR chemical shifts for the imidazolium cation, we have conducted a series of benchmark calculations on the C1mim cation. The C_{2v} structure and atom labeling of C1mim are presented in Figure 1. We consider relative chemical shifts of the C1mim

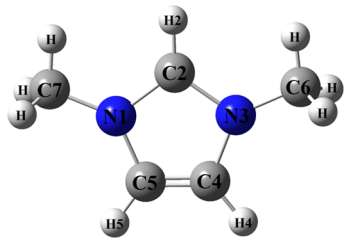

Figure 1. 1,3-Dimethylimidazolium cation, C1mim.

cation here as these are easier to compute accurately due to the apparent cancellation of errors, as opposed to the isotropic shielding constants. Because our QM/MM calculations of NMR chemical shifts will be performed at the DFT level of theory, we have selected the PBE0 functional for the basis set analysis of the relative chemical shifts, and the results are collected in Table 1. The relative ^{1}H NMR chemical shifts for

Table 1. Relative ^{1}H NMR Chemical Shifts (in ppm) for the C1mim Cation Calculated Using the PBE0 Functional and Different Basis Sets[a]

basis set	H2	H4/5
def2-SVP(143)	3.50	3.47
def2-SVPD(228)	3.79	3.48
def2-TZVP(271)	3.88	3.61
def2-TZVPD(340)	3.99	3.57
def2-QZVP(669)	3.91	3.58
def2-QZVPD(738)	3.93	3.57
aug-cc-pVDZ(242)	3.88	3.52
aug-cc-pVTZ(529)	3.94	3.56
aug-cc-pVQZ(947)	3.91	3.55
aug-cc-pCVDZ(270)	3.86	3.52
aug-cc-pCVTZ(620)	3.92	3.55
aug-cc-pCVQZ(1177)	3.90	3.55

[a]The number of contracted basis functions is indicated in parentheses for each basis.

H2 and H4/5 protons are evaluated with respect to the arithmetic average of the protons in the methyl group of C1mim. As seen in Table 1, the relative chemical shifts are apparently well converged for the most extensive basis set we have used, which is aug-cc-pCVQZ. The effect of tight core functions included in the Dunning-type basis sets is rather

https://dx.doi.org/10.1021/acs.jpcb.0c07450
J. Phys. Chem. B 2020, 124, 10776−10786

small for relative shifts. In general, we see that reasonable results for the relative ^{1}H NMR chemical shifts can be expected with all basis sets but Ahlrich's single valence-type basis sets, thus corroborating the findings in ref 105. Owing to the size of the C10mim cation, we have chosen the def2-TZVP basis set for our subsequent calculations of NMR isotropic shielding constants, a choice that has proven appropriate for NMR properties of other organic molecules in the liquid phases.[70,76]

The relative ^{1}H NMR chemical shifts of the C1mim cation computed using three different DFT functionals as well as the MP2 and CCSD approaches combined with the def2-TZVP basis set are collected in Table 2. Interestingly, we have found

Table 2. Relative ^{1}H NMR Chemical Shifts (in ppm) for the C1mim Cation Calculated Using Different Electronic Structure Methods along with the def2-TZVP Basis Set

method	H2	H4/5
PBE0	3.88	3.61
B3LYP	3.83	3.54
KT3	3.69	3.48
MP2	3.65	3.59
CCSD	3.89	3.57

considerable differences between the relative chemical shifts for H2 proton computed using the correlated *ab initio* MP2 and CCSD methods. The PBE0 functional is seen to provide relative chemical shifts that are closest to the corresponding CCSD predictions. On these grounds, we have chosen the PBE0 exchange−correlation functional along with the def2-TZVP basis set for all further calculations of NMR isotropic shielding constants in this work.

Classical MD Simulations. Classical MD simulations of a single [C10mim][Cl] contact ion pair forming a hydrogen bond through the C2−H2 bond of the imidazolium ring have been pursued in aqueous as well as in ACN and DCM solutions. The C2−H2 moiety has been recognized as the primary site for hydrogen bonding of the imidazolium cation,[36,64,65] and thus, we have excluded the configuration of the ionic pair where the hydrogen bonding between the ions is formed through the C4−H4 or the C5−H5 bonds from consideration. We have observed the [C10mim][Cl] ion pair to disrupt in water already during the early stages of the equilibration, meaning that present force fields predict the fully dissociated state of [C10mim][Cl] IL at infinite dilution in an aqueous solution, in line with the findings in refs 35, 37−41. The contact ion pair remained intact in the other two less polar solvents, and the most probable distance between the H2 proton and Cl^- anion was found to be around 2.53 Å in both DCM and ACN. In Figure 2a, we show the distribution of the hydrogen bond angle C2−H2···Cl^- in ACN and DCM. We readily observe that the C2−H2···Cl^- hydrogen bond is strongly nonlinear, and we generally find the hydrogen bond angles to be smaller in ACN rather than in DCM. The most probable hydrogen bond angle is around 130° in ACN and around 150° in DCM. The distribution of the dihedral angle N1−C2−H2···Cl^- shown in Figure 2b illustrates quite clearly that the chloride anion tends to be located out of the plane of the imidazolium ring with roughly the same probability of being on either side of it in both solvents. In addition, the anion is seen to have the preference for leaning more toward the methyl rather than the decyl group side, apparently, due to the steric effects. Our findings are thus in contradiction to those based on the quantum chemical geometry optimization of the isolated ion pair composed of an imidazolium cation and a chloride anion. These computations predict two configurations of the ion pair with comparable interaction energies where the chloride is positioned either in the plane of the imidazolium ring forming almost a linear hydrogen bond or on top of the C2−H2 bond.[78,106,107] Car−Parinello MD simulations of the neat [C2mim][Cl] IL indicate the C2−H2···Cl^- to be preferably linear,[78] while those of the [C2mim][Cl] ion pair in aqueous solution show reasonable populations of configurations with chloride being both in-plane of the imidazolium ring and on top of the C2−H2 bond with a preference for the former.[108] However, classical MD simulations of mixtures of [C4mim][Cl] IL with water and DMSO reported in ref 37 also find the distribution of chloride around the C2−H2 bond to be qualitatively similar to that of the present study. Classical MD simulations of neat [C4mim][Cl] IL lead to qualitatively different results concerning the preferred location of the chloride anions around the C2−H2 moiety, apparently depending on the used force field.[78,109] Interestingly, the neutron scattering measurements of neat [C2mim][Cl] IL have shown that the most probable C2−H2···Cl^- hydrogen bond angle corresponds to the position of the chloride anion that is intermediate between the in-plane and on top of the C2−H2 bond configurations.[110]

In Figure 3, we show the radial distribution functions, RDFs, between the H2 atom of the free C10mim cation and the electronegative atoms in the molecules of each of the three

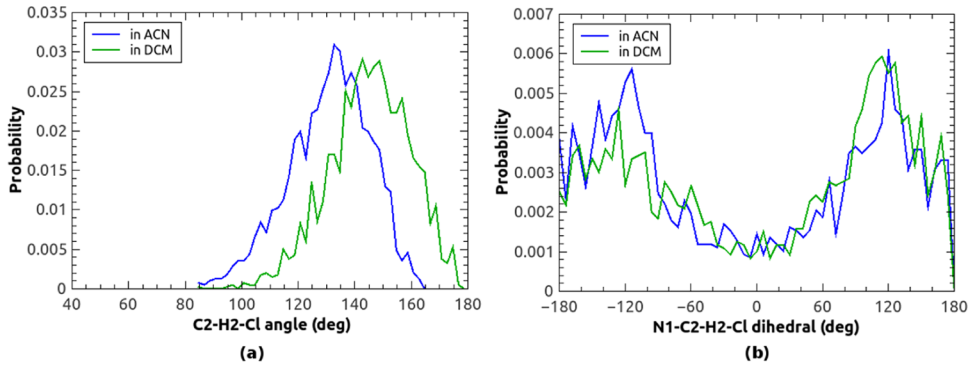

Figure 2. Distribution of the C2−H2···Cl^- (a) and the dihedral N1−C2−H2···Cl^- (b) angle around the C2−H2 moiety of the imidazolium ring in ACN and DCM.

https://dx.doi.org/10.1021/acs.jpcb.0c07450
J. Phys. Chem. B 2020, 124, 10776−10786

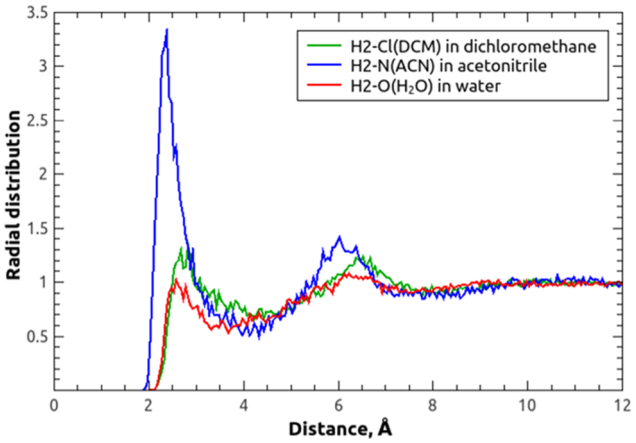

Figure 3. RDFs between the H2 atom of the free C10mim cation and the electronegative atoms of the solvent molecules.

solvents: the oxygen atom of water, the nitrogen atom of ACN, and chlorine atoms of DCM. These RDFs were recorded during our simulations of dissociated [C10mim][Cl] ion pairs. The RDFs indicate some association of the C10mim cation with the solvent molecules through the C2−H2 bond of the imidazolium ring. Spherical integration of the first peaks in the RDFs in Figure 3 gives an average number of corresponding atoms of the solvent molecules in the vicinity of the C2−H2 moiety. These numbers were found to be 3.7, 2.9, and 3.6 in DCM, ACN, and aqueous solution, respectively. The spherical integration of the first peak of the RDF between H2 atom of imidazolium and carbon atom of DCM molecules extended up to 5.23 Å results in the coordination number of 2.8. Thereby, we barely see any specific interactions between the C10mim cations and rather nonpolar DCM molecules.

To scrutinize the local distribution of the solvent molecules around the C2−H2 bond in the C10mim cation in some more detail, we have analyzed the distributions of the C2−H2···X angle and the N1−C2−H2···X dihedral angle, where X corresponds to the O, N, or Cl atoms in water, ACN, or DCM molecules, respectively, see Figure 4. These distributions have been compiled by considering only those solvent molecules for which the distance between the H2 atom and O atom of water, N atom of ACN, and Cl atoms of DCM does not exceed 3.7, 4.3, and 4.4 Å, respectively. These cutoff values are based on the RDFs shown in Figure 3. As seen in Figure 4a, the angular distribution peaks at around 130°. We also find that the solvent molecules,—in particular, those of ACN and DCM solvents and somewhat less those of water,—tend to be located above the imidazolium ring within the applied thresholds for the interatomic distances. The distributions of dihedrals shown in Figure 4b mimic the distribution of corresponding dihedral angles between the cation and the anion in the [C10mim][Cl] contact ion pair shown in Figure 2b, indicating again that solvent molecules tend to be positioned out of the imidazolium ring plane.

NMR Results. The QM/MM results for the ^{1}H NMR isotropic shielding constants of the H2 proton in the imidazolium ring of the solvated C10mim cation are presented in Table 3. Each entry for the shielding constant in Table 3 is obtained as an average over 100 molecular configurations recorded during the MD simulation. For the free C10mim cation in aqueous solution, we have computed the NMR shieldings using two types of the classical potential for all water molecules—the nonpolarizable TIP3P as well as a polarizable potential due to Ahlström et al.[104] The latter potential includes isotropic molecular dipole polarizability assigned to the oxygen atom in addition to the three partial atomic point charges. As seen in Table 3, the results for the shielding constant of the H2 proton computed using both potentials are virtually identical, and we have thus chosen to use nonpolarizable potentials for all classical solvent molecules of water, ACN, and DCM in all subsequent QM/MM calculations.

In the QM/MM scheme utilizing nonpolarizable potentials, the inclusion of some of the solvent molecules to the quantum mechanically treated region of the model offers an improved description of electrostatic interactions between the solute and the solvent. In addition, mutual solute−solvent polarization as well as nonclassical effects such as Pauli repulsion are introduced. It is typically mandatory to treat the solvent molecules forming the hydrogen bonds with the solute using the QM approach rather than to describe them by a classical potential, so that both the hydrogen bond donor and acceptor molecules are considered on an equal footing.[69−71,73,74] We have considered here the expansion of the QM part of the model by a few relevant solvent molecules as well as chloride anion in the case of the simulated contact ion pair. We have thus included up to three molecular species closest to the H2 atom to the region of the model treated quantum mechanically by DFT. In addition, two solvent molecules closest to the H4 and H5 atoms were also promoted to the QM part to make sure all hydrogen-bonding interactions involving the imidazolium ring of C10mim are accounted for consistently. As seen in

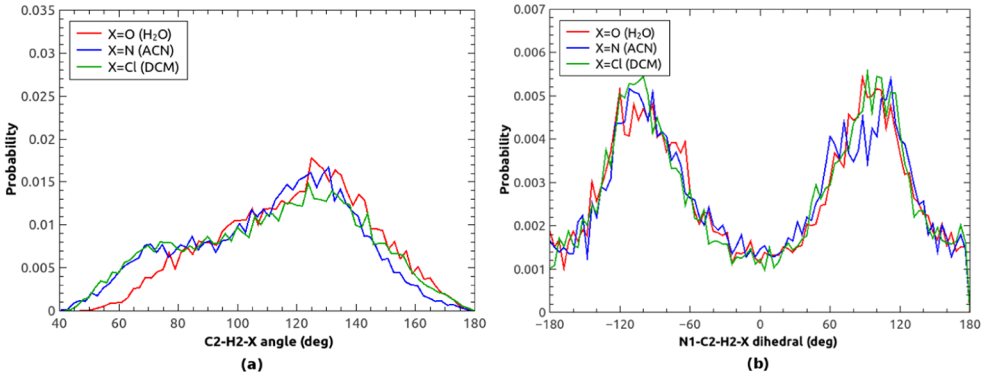

Figure 4. Distribution of the C2−H2···X (a) and the dihedral N1−C2−H2···X (b) angle, where X is the electronegative atom in the solvent molecules found in the vicinity of the C2−H2 bond of free C10mim cation. See the text for details.

https://dx.doi.org/10.1021/acs.jpcb.0c07450
J. Phys. Chem. B 2020, 124, 10776−10786

Table 3. Statistically Averaged NMR Isotropic Shielding Constants, σ, (in ppm) of the H2 Proton of the C10mim Cation in Water, ACN, and DCM Computed Using the PBE0/def2-TZVP Level of Theory[b]

system	QM region	σ(H2)
FI in water	C10mim	23.64 (0.07)
	C10mim[a]	23.62 (0.07)
	C10mim (1,1,1)	23.31 (0.08)
	C10mim (3,0,0)	23.06 (0.08)
	C10mim (3,1,1)	23.08 (0.09)
FI in ACN	C10mim	23.62 (0.03)
	C10mim (1,1,1)	23.09 (0.05)
	C10mim (3,0,0)	22.98 (0.05)
	C10mim (3,1,1)	23.00 (0.05)
CP in ACN	C10mim	23.30 (0.04)
	C10mim (2,1,1)	21.44 (0.08)
	C10mim (3,0,0)	21.48 (0.08)
	C10mim (3,1,1)	21.50 (0.08)
FI in DCM	C10mim	24.02 (0.03)
	C10mim (1,1,1)	23.52 (0.06)
	C10mim (3,0,0)	23.36 (0.06)
	C10mim (3,1,1)	23.41 (0.06)
CP in DCM	C10mim	23.23 (0.03)
	C10mim (2,1,1)	21.29 (0.09)
	C10mim (3,0,0)	21.29 (0.08)
	C10mim (3,1,1)	21.33 (0.08)

[a]Computed using the polarizable potential for water molecules.[104] [b]Statistical errors are evaluated as standard deviations of the sample and are provided in parentheses. The state of the [C10mim][Cl] ion pair in the system is indicated as FI for free ions or CP for contact ion pair. In the second column, the three integers given in parentheses indicate the numbers of solvent molecules—including chloride in the case of the CP—promoted to the QM region closest to H2, H4, and H5 atoms, respectively.

Table 3, 3 solvent molecules—or two solvent molecules plus the anion in the case of the contact ion pair—is a sufficient expansion of the QM region to obtain a converged effect on the shielding constant of the H2 atom. However, the quantum mechanical treatment of hydrogen bonding between solvent molecules and imidazolium cation through the C4−H4 and C5−H5 bonds has apparently a very small effect on the shielding constant of the H2 proton.

The improved description of intermolecular interactions has a marked effect on the shielding constant of the H2 proton. In the case of the free C10mim cation, the shielding constant is decreased by around 0.5−0.6 ppm as compared to the case where only the cation is considered at the DFT level and all solvent molecules are represented by the point charge potential, for all three solutions. The effect is even stronger for the contact ion pair. Here, the shielding constant of the H2 atom decreases by 1.8−1.9 ppm compared to the case where both the anion and all solvent molecules are represented by the potential. As seen in Table 3, the hydrogen bonding between the C10mim cation and the chloride anion has a significant modulating effect on the magnitude of the shielding constant of the H2 atom, while hydrogen bonding between C10mim and solvent molecules as well as the polarity of the solvent is clearly of less importance. Indeed, the formation of the contact ion pair leads to the deshielding of the H2 atom by 1.5 and 2.1 ppm compared to the corresponding shielding constant of the free cation in ACN and DCM solution, respectively. However, the shielding constants of the H2 atom for the contact ion pair differ by a mere 0.17 ppm in ACN and DCM solution. The shieldings of H2 proton for the free C10mim are virtually identical in ACN and water, and it is somewhat larger in DCM by around 0.4 ppm.

In Table 4, we have collected our computational predictions for the ^{1}H NMR chemical shifts of the H2 atom in the

Table 4. NMR Chemical Shifts, δ, (in ppm) of the H2 Proton in the Imidazolium Ring of the C10mim Cation in Water, ACN, and DCM Evaluated with Respect to TMS[a]

system	δ(H2)
FI in water	8.83
FI in ACN	8.91
CP in ACN	10.41
FI in DCM	8.50
CP in DCM	10.58
expmnt. (water)	8.66
expmnt. (ACN)	9.23
expmnt. (DCM)	10.83

[a]Chemical shifts are based on the ^{1}H NMR shielding constants computed using the most extensive QM region in this work. FI and CP indicate free ions and contact ion pair, respectively. Experimental data is provided at the end of the table.

[C10mim][Cl] contact ion pair and in the free C10mim cation in the solutions of water, ACN, and DCM. These results are based on the isotropic shielding constants of the H2 proton calculated using the most extensive QM region in the QM/MM calculations as given in Table 3. The chemical shifts were evaluated with respect to the shielding constant of equivalent protons in TMS. The geometry of the isolated TMS has been here optimized at the Hartree−Fock level together with the 6-31+G* basis set to be consistent with the protocol adopted for the development of the AMBER type force field for the C10mim cation applied in the MD simulations.[83] The shielding constant for the protons of TMS of 31.91 ppm was then obtained using the PBE0 exchange−correlation functional and the def2-TZVP basis set. Our experimental results for the NMR chemical shifts of the H2 atom of [C10mim][Cl] IL solutions in water, ACN, and DCM are also included in Table 4.

The QM/MM result for the chemical shift of the H2 proton in the free C10mim cation in an aqueous solution of 8.83 ppm compares very well to the experimental shift of 8.66 ppm measured for the sample of the [C10mim][Cl] aqueous solution, where the molar fraction of the IL is equal to 10^{-5}. This finding lends strong support to the notion that [C10mim][Cl] IL completely dissociates into free fully solvated ions in aqueous solutions at these very low concentrations. In ACN, the experimental chemical shift is found to be in-between those computed for the contact ion pair and for the free C10mim cation, being closer to the latter. Assuming that chemical equilibrium in ACN is established only between the dissociated state of the ions and the contact ion pairs formed via hydrogen bonding solely through the C2−H2 bond of the imidazolium ring, we can evaluate the fraction of the contact ion pairs, X^{CP}_{ACN}, according to

$$X^{CP}_{ACN} = \frac{\delta^{exp}_{ACN} - \delta^{FI}_{ACN}}{\delta^{CP}_{ACN} - \delta^{FI}_{ACN}} \quad (1)$$

In eq 1, CP and FI indicate the contact ionic pair and free C10mim cation, respectively. Using data in Table 4, we find

https://dx.doi.org/10.1021/acs.jpcb.0c07450
J. Phys. Chem. B 2020, 124, 10776−10786

X_{ACN}^{CP} to be equal to 0.23, meaning that on average one ion pair out of four or five is found in the aggregated state. We thus conclude that acetonitrile is in fact able to break the contact ion pairs of the [C10mim][Cl] IL apart and the equilibrium is shifted toward the free fully solvated ions at molar fractions of the IL as low as 10^{-5}. Apparently, the driving force behind this phenomenon is the ability of the ACN molecules to form hydrogen bonding with the C10mim cation, even though ACN molecules do not possess strong hydrogen-bond donating abilities to solvate chloride anions efficiently.

As seen in Table 4, the NMR chemical shift of the H2 atom measured for the sample of the [C10mim][Cl] solution in DCM is higher than our QM/MM prediction for the chemical shift of this atom in the cation−anion contact ion pair by 0.25 ppm. Our findings thus indicate that dissociation of the [C10mim][Cl] IL into free ions does not occur in the rather nonpolar DCM solution even at this extremely low concentration of the IL. On the one hand, the discrepancy between experimental measurements and computational predictions in the DCM solution may be due to the inaccuracies of the applied computational scheme. On the other hand, experimental findings indicate that the ions of the [C10mim][Cl] IL may form larger ionic aggregates rather than separate contact ion pairs in DCM. The adopted computational procedure cannot provide an unambiguous conclusion regarding the latter possibility, but we have undertaken measures to get a feeling of the accuracy of our computational procedure based on the integrated MD-QM/MM approach. It has been demonstrated that the accuracy of the NMR chemical shifts modeled using the QM/MM scheme along with the MD simulations based on flexible force fields may suffer from an inherently incorrect sampling of the vibrational phase space due to the imperfections in the classical force field.[71] An alternative approach to predict molecular properties of solvated molecules is the supermolecular approach, where specific interactions between the solute and the solvent are accounted for by geometry-optimizing small solute−solvent molecular aggregates along with the PCM model to account for the bulk solvent effects. This approach allows for comparatively more accurate molecular geometries that are indeed important as much as NMR chemical shifts are concerned. However, the energy-minimized structure of the molecular aggregate does represent only one point on the molecular potential energy hypersurface meaning that the dynamical solute−solvent effects remain here completely neglected.

In Table 5, we have collected the calculated NMR chemical shifts of the H2 atom for the geometry-optimized C10mim cation and its complexes with water, ACN, and DCM molecules as well as with the chloride anion. Geometry optimizations have been carried out at the B3LYP/6-31++G** level of the theory along with the PCM to account for bulk solvent effects. We only consider the hydrogen-bonded complexes formed through the C2−H2 moiety of the imidazolium ring. The optimized complexes are illustrated in Figure 5. Contrary to the case of the isolated ion pair,[106,107] the configuration of the [C10mim][Cl] aggregate where the chloride anion is situated on top of the C2−H2 bond is not a minimum on the potential energy surface when PCM is applied, and it evolves down to the configuration with the chloride in the plane of the imidazolium ring as shown in Figure 5D. NMR chemical shifts given in Table 5 have been evaluated with respect to the ^{1}H NMR isotropic shielding constant of TMS of 31.62 ppm computed using the geometry of TMS optimized at the same level of theory as the molecular complexes under investigation.

Table 5. Supermolecular Results for the NMR Chemical Shifts, δ, (in ppm) of the H2 Proton of the C10mim Cation and Its Aggregates with Water, ACN, and DCM Molecules as well as with Chloride Computed Using PBE0/def2-TZVP/PCM Level of Theory

system	δ(H2)
C10mim in water	8.03
C10mim + H_2O in water	10.02
C10mim in ACN	8.03
C10mim + ACN in ACN	9.05
C10mim + Cl in ACN	11.44
C10mim in DCM	8.00
C10mim + DCM in DCM	8.37
C10mim + Cl in DCM	12.20

We immediately observe that the chemical shift of the H2 atom in the C10mim cation is virtually the same in all three solvents if lone C10mim cation is immersed in the PCM cavity. The inclusion of the hydrogen-bonded solvent molecule has, however, a very large effect on the chemical shift of the H2 proton, leading to additional deshielding by around 2 and 1 ppm in water and ACN, respectively. Even though DCM has weak hydrogen-bond accepting abilities, the shielding constant of the H2 atom in the complex of the C10mim cation and DCM molecule is increased by a substantial ∼0.4 ppm as compared to the case where the DCM solvent is represented entirely by the dielectric continuum. The chemical shift of the H2 atom in the complex of the C10mim cation with the water molecule of 10.02 ppm is considerably overestimated as compared to the experimental chemical shift of 8.66 ppm measured for the aqueous solution of the [C10mim][Cl] IL. In ACN, the supermolecular approach predicts the equilibrium to be shifted toward the free ions rather than contact ion pairs even more so than that based on the MD-QM/MM scheme. The experimental chemical shift of the H2 atom of 10.83 ppm measured for the [C10mim][Cl] solution in DCM is situated roughly in the middle of the corresponding chemical shifts predicted for the complexes of C10mim with the chloride anion and DCM molecule, suggesting ample dissociation of the [C10mim][Cl] in the DCM solution. This conclusion is inconsistent with the experimental findings as well as with the predictions based on the MD-QM/MM approach.

Comparing the results of these two approaches, we conclude that it is mandatory to account for the dynamics of the solvent as well as of the chloride anion around the imidazolium cation to obtain a qualitatively correct picture of the NMR spectra of IL systems, as also stressed in ref 78. The supermolecular approach is based on the static energy-minimized solute−solvent structures may not be a sufficiently accurate representation of the solute−solvent and, particularly, for ILs, of the cation−anion interactions. The supermolecular approach has been applied to predict NMR properties of IL systems,[64,105,111] yet the results should be seen with a degree of caution.

CONCLUSIONS

In this work, the pairing of the constituent ions of the [C10mim][Cl] ionic liquid in its low-concentration solutions in solvents of different polarities and different capabilities for hydrogen bonding is addressed. The ^{1}H NMR chemical shifts

https://dx.doi.org/10.1021/acs.jpcb.0c07450
J. Phys. Chem. B 2020, 124, 10776−10786

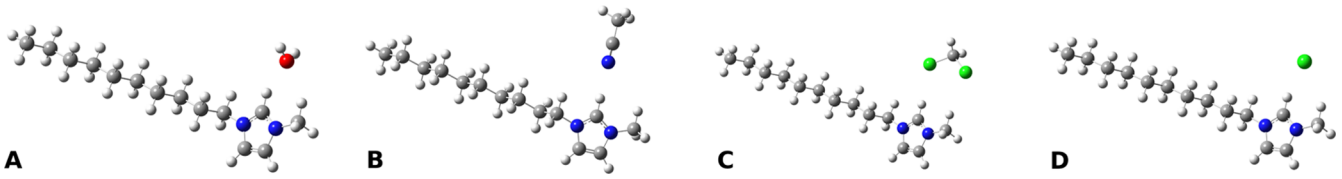

Figure 5. Energy-minimized complexes of the C10mim cation with water (A), ACN (B), DCM (C) molecules as well as the chloride anion (D).

of the H2 proton have been measured for the sample of [C10mim][Cl] solutions in water, acetonitrile, and dichloromethane where the molar fraction of the IL is as low as 10^{-5}. To rationalize experimental data, we have conducted classical MD simulations of a single contact ion pair as well as of the system where the ion pair is dissociated into free ions in all three solvents. The QM/MM approach based on DFT and nonpolarizable potentials was then used to calculate the NMR isotropic shielding constants of the H2 proton of the C10mim cation forming the contact pair with the anion and in its free fully solvated state. We assume that the equilibrium is established only between the contact ion pairs linked by the hydrogen bonding through the C2−H2 moiety and the free ions at these low concentrations of the ionic liquid. Combining measured and calculated NMR chemical shifts of the H2 atom, we can quantify the fraction of the ions forming contact pairs in the solution.

Classical MD simulations suggest that the [C10mim][Cl] ionic liquid breaks into free ions in aqueous solutions completely, and the modeled NMR chemical shift of the H2 atom of the free C10mim cation in aqueous solutions is found to agree well with the experimental value. In acetonitrile, around 23% of the ion pairs were found to form contact pairs and the rest are broken into free ions. Modeling suggests that ion-pair dissociation does not take place in the nonpolar dichloromethane solvent. As predicted by the QM/MM model, the chemical shift of the H2 atom in the C10mim cation is primarily modulated by hydrogen bonding to the chloride anion, while the effect of the solvent is rather small. Chemical shifts of the H2 proton have a very similar value for the free C10mim cation in all three solutions and likewise for the contact ion pair in acetonitrile and dichloromethane. We have also attempted the supermolecular approach to predict the NMR chemical shifts of the H2 atom in C10mim, but we find the results to be inferior to those based on the MD-QM/MM scheme.

AUTHOR INFORMATION

Corresponding Author

Kęstutis Aidas − *Institute of Chemical Physics, Faculty of Physics, Vilnius University, LT-10257 Vilnius, Lithuania;* orcid.org/0000-0003-1359-3573; Phone: +370 5 223 4593; Email: kestutis.aidas@ff.vu.lt

Authors

Dovilė Lengvinaitė − *Institute of Chemical Physics, Faculty of Physics, Vilnius University, LT-10257 Vilnius, Lithuania*

Vytautas Klimavičius − *Institute of Chemical Physics, Faculty of Physics, Vilnius University, LT-10257 Vilnius, Lithuania; Eduard-Zintl Institute for Inorganic and Physical Chemistry, University of Technology Darmstadt, D-64287 Darmstadt, Germany*

Vytautas Balevicius − *Institute of Chemical Physics, Faculty of Physics, Vilnius University, LT-10257 Vilnius, Lithuania;* orcid.org/0000-0002-3770-1471

Complete contact information is available at: https://pubs.acs.org/10.1021/acs.jpcb.0c07450

Notes

The authors declare no competing financial interest.

ACKNOWLEDGMENTS

This work is supported by the Research Council of Lithuania, Grant no. S-MIP-17-84. Computations have been conducted on the resources provided by the High Performance Computing Center "HPC Saulėtekis" at the Faculty of Physics, Vilnius University. Computational resources provided by the Swedish National Infrastructure for Computing (SNIC) at HPC2N are also acknowledged.

REFERENCES

(1) Welton, T. Room-Temperature Ionic Liquids. Solvents for Synthesis and Catalysis. *Chem. Rev.* **1999**, *99*, 2071−2083.
(2) Hayes, R.; Warr, G. G.; Atkin, R. Structure and Nanostructure in Ionic Liquids. *Chem. Rev.* **2015**, *115*, 6357−6426.
(3) Weingärtner, H. Understanding Ionic Liquids at the Molecular Level: Facts, Problems, and Controversies. *Angew. Chem., Int. Ed.* **2008**, *47*, 654−670.
(4) Wang, Y.-L.; Li, B.; Sarman, S.; Mocci, F.; Lu, Z.-Y.; Yuan, J.; Laaksonen, A.; Fayer, M. D. Microstructural and Dynamical Heterogeneities in Ionic Liquids. *Chem. Rev.* **2020**, *120*, 5798−5877.
(5) Swatloski, R. P.; Spear, S. K.; Holbrey, J. D.; Rogers, R. D. Dissolution of Cellose with Ionic Liquids. *J. Am. Chem. Soc.* **2002**, *124*, 4974−4975.
(6) Somers, A. E.; Howlett, P. C.; MacFarlane, D. R.; Forsyth, M. A Review of Ionic Liquid Lubricants. *Lubricants* **2013**, *1*, 3−21.
(7) Zakeeruddin, S. M.; Grätzel, M. Solvent-Free Ionic Liquid Electrolytes for Mesoscopic Dye-Sensitized Solar Cells. *Adv. Funct. Mater.* **2009**, *19*, 2187−2202.
(8) Bates, E. D.; Mayton, R.; Ntai, I.; Davis, J. H. CO_2 Capture by a Task-Specific Ionic Liquid. *J. Am. Chem. Soc.* **2002**, *124*, 926−927.
(9) Hasib-ur-Rahman, M.; Siaj, M.; Larachi, F. Ionic liquids for CO_2 capture − Development and progress. *Chem. Eng. Process.* **2010**, *49*, 313−322.
(10) Visser, A. E.; Swatloski, R. P.; Reichert, W. M.; Mayton, R.; Sheff, S.; Wierzbicki, A.; Davis, J. H., Jr.; Rogers, R. D. Task-Specific Ionic Liquids for the Extraction of Metal Ions from Aqueous Solutions. *Chem. Commun.* **2001**, *0*, 135−136.
(11) Janssen, C. H. C.; Macías-Ruvalcaba, N. A.; Aguilar-Martínez, M.; Kobrak, M. N. Metal Extraction to Ionic Liquids: the Relationship between Structure, Mechanism and Application. *Int. Rev. Phys. Chem.* **2015**, *34*, 591−622.
(12) Blanchard, L. A.; Hancu, D.; Beckman, E. J.; Brennecke, J. F. Green Processing using Ionic Liquids and CO_2. *Nature* **1999**, *399*, 28−29.
(13) Tzschucke, C. C.; Markert, C.; Bannwarth, W.; Roller, S.; Hebel, A.; Haag, R. Modern Separation Techniques for the Efficient Workup in Organic Synthesis. *Angew. Chem., Int. Ed* **2002**, *41*, 3964−4000.
(14) Han, D.; Row, K. H. Recent Applications of Ionic Liquids in Separation Technology. *Molecules* **2010**, *15*, 2405−2426.
(15) Welton, T.; Wasserscheid, P. *Ionic Liquids and Synthesis*; Wiley-VCH: Weinheim, 2002.

(16) Hallett, J. P.; Welton, T. Room-Temperature Ionic Liquids: Solvents for Synthesis and Catalysis. 2. *Chem. Rev.* **2011**, *111*, 3508−3576.
(17) Welton, T. Ionic Liquids in Catalysis. *Coord. Chem. Rev.* **2004**, *248*, 2459−2477.
(18) Wilkes, J. S. Properties of Ionic Liquid Solvents for Catalysis. *J. Mol. Catal. A: Chem.* **2004**, *214*, 11−17.
(19) Hajipour, A. R.; Refiee, F. Recent Progress in Ionic Liquids and their Applications in Organic Synthesis. *Org. Prep. Proced. Int.* **2015**, *47*, 249−308.
(20) Lu, J.; Yan, F.; Texter, J. Advanced Applications of Ionic Liquids in Polymer Science. *Prog. Polym. Sci.* **2009**, *34*, 431−448.
(21) Lu, W.; Fadeev, A. G.; Qi, B.; Smela, E.; Mattes, B. R.; Ding, J.; Spinks, G. M.; Mazurkiewicz, J.; Zhou, D.; Wallace, G. G.; et al. Use of Ionic Liquids for π-Conjugated Polymer Electrochemical Devices. *Science* **2002**, *297*, 983−987.
(22) Tiruye, G. A.; Muñoz-Torrero, D.; Palma, J.; Anderson, M.; Marcilla, R. All-Solid State Supercapacitors Operating at 3.5 V by using Ionic Liquid based Polymer Electrolytes. *J. Power Sources* **2015**, *279*, 472−480.
(23) Fernicola, A.; Scrosati, B.; Ohno, H. Potentialities of Ionic Liquids as new Electrolyte Media in Advanced Electrochemical Devices. *Ionics* **2006**, *12*, 95−102.
(24) Kohno, Y.; Ohno, H. Ionic Liquid/Water Mixtures: from Hostility to Conciliation. *Chem. Commun.* **2012**, *48*, 7119−7130.
(25) Fujita, K.; MacFarlane, D. R.; Forsyth, M. Protein Solubilising and Stabilising Ionic Liquids. *Chem. Commun.* **2005**, *99*, 4804−4806.
(26) Fujita, K.; Forsyth, M.; MacFarlane, D. R.; Reid, R. W.; Elliott, G. D. Unexpected Improvement in Stability and Utility of Cytochrome c by Solution in Biocompatible Ionic Liquids. *Biotechnol. Bioeng.* **2006**, *94*, 1209−1213.
(27) Nanda, R. Unusual Linear Dependency of Viscosity with Temperature in Ionic Liquid/Water Mixtures. *Phys. Chem. Chem. Phys.* **2016**, *18*, 25801−25805.
(28) Gómez, E.; González, B.; Domínguez, A.; Tojo, E.; Tojo, J. Dynamic Viscosities of a Series of 1-Alkyl-3-methylimidazolium Chloride Ionic Liquids and Their Binary Mixtures with Water at Several Temperatures. *J. Chem. Eng. Data* **2006**, *51*, 696−701.
(29) Seddon, K. R.; Stark, A.; Torres, M.-J. Influence of Chloride, Water, and Organic Solvents on the Physical Properties of Ionic Liquids. *Pure Appl. Chem.* **2000**, *72*, 2275−2287.
(30) Stoppa, A.; Hunger, J.; Buchner, R. Conductivities of Binary Mixtures of Ionic Liquids with Polar Solvents. *J. Chem. Eng. Data* **2009**, *54*, 472−479.
(31) Buzzeo, M. C.; Hardacre, C.; Compton, R. G. Extended Electrochemical Windows Made Accessible by Room Temperature Ionic Liquid/Organic Solvent Electrolyte Systems. *ChemPhysChem* **2006**, *7*, 176−180.
(32) Najafabadi, A. T.; Gyenge, E. High-Yield Graphene Production by Electrochemical Exfoliation of Graphite: Novel Ionic Liquid (IL)-Acetonitrile Electrolyte with low IL Content. *Carbon* **2014**, *71*, 58−69.
(33) Matsubara, Y.; Grills, D. C.; Kuwahara, Y. Thermodynamic Aspects of Electrocatalytic CO_2 Reduction in Acetonitrile and with an Ionic Liquid as Solvent or Electrolyte. *ACS Catal.* **2015**, *5*, 6440−6452.
(34) Stassen, H. K.; Ludwig, R.; Wulf, A.; Dupont, J. Imidazolium Salt Ion Pairs in Solution. *Chem. - Eur. J.* **2015**, *21*, 8324−8335.
(35) Boruń, A. Conductance and Ionic Association of Selected Imidazolium Ionic Liquids in Various Solvents: A Review. *J. Mol. Liq.* **2019**, *276*, 214−224.
(36) Köddermann, T.; Wertz, C.; Heintz, A.; Ludwig, R. Ion-Pair Formation in the Ionic Liquid 1-Ethyl-3-methylimidazolium Bis-(triflyl)imide as a Function of Temperature and Concentration. *ChemPhysChem* **2006**, *7*, 1944−1949.
(37) Remsing, R. C.; Liu, Z.; Sergeyev, I.; Moyna, G. Solvation and Aggregation of N,N'-Dialkylimidazolium Ionic Liquids: A Multinuclear NMR Spectroscopy and Molecular Dynamics Simulation Study. *J. Phys. Chem. B* **2008**, *112*, 7363−7369.
(38) Ma, C.; Laaksonen, A.; Liu, C.; Lu, X.; Ji, X. The Peculiar Effect of Water on Ionic Liquids and Deep Eutectic Solvents. *Chem. Soc. Rev.* **2018**, *47*, 8685−8720.
(39) Cha, S.; Ao, M.; Sung, W.; Moon, B.; Ahlström, B.; Johansson, P.; Ouchid, Y.; Kim, D. Structures of Ionic Liquid-Water Mixtures Investigated by IR and NMR Spectroscopy. *Phys. Chem. Chem. Phys.* **2014**, *16*, 9591−9601.
(40) Pierola, I. F.; Agzenai, Y. I. Pairing and Anion-Driven Aggregation of an Ionic Liquid in Aqueous Salt Solutions. *J. Phys. Chem. B* **2012**, *116*, 3973−3981.
(41) Giesecke, M.; M'eriguet, G.; Hallberg, F.; Fang, Y.; Stilbs, P.; Furó, I. Ion Association in Aqueous and non-Aqueous Solutions Probed by Diffusion and Electrophoretic NMR. *Phys. Chem. Chem. Phys.* **2015**, *17*, 3402−3408.
(42) Gutiérrez, A.; Atilhan, M.; Alcalde, R.; Trenzado, J. L.; Aparicio, S. Insights on the Mixtures of Imidazolium based Ionic Liquids with Molecular Solvents. *J. Mol. Liq.* **2018**, *255*, 199−207.
(43) Wang, H.; Liu, M.; Zhao, Y.; Xuan, X.; Zhao, Y.; Wang, J. Hydrogen Bonding Mediated Ion Pairs of some Aprotic Ionic Liquids and their Structural Transition in Aqueous Solution. *Sci. China Chem.* **2017**, *60*, 970−978.
(44) Dupont, J.; Suarez, P. A. Z.; De Souza, R. F.; Burrow, R. A.; Kintzinger, J.-P. C-H-π Interactions in 1-*n*-Butyl-3-methylimidazolium Tetraphenylborate Molten Salt: Solid and Solution Structures. *Chem. - Eur. J.* **2000**, *6*, 2377−2381.
(45) Zhou, Y.; Gong, S.; Xu, X.; Yu, Z.; Kiefer, J.; Wang, Z. The Interactions between Polar Solvents (Methanol, Acetonitrile, Dimethylsulfoxide) and the Ionic Liquid 1-Ethyl-3-Methylimidazolium bis(fluorosulfonyl)imide. *J. Mol. Liq.* **2020**, *299*, No. 112159.
(46) Zheng, Y.-Z.; Zhou, Y.; Deng, G.; Yu, Z.-W. Hydrogen-Bonding Interactions between a Nitrile-Based Functional Ionic Liquid and DMSO. *J. Mol. Struct.* **2016**, *1124*, 207−215.
(47) Fumino, K.; Stange, P.; Fossog, V.; Hempelmann, R.; Ludwig, R. Equilibrium of Contact and Solvent-Separated Ion Pairs in Mixtures of Protic Ionic Liquids and Molecular Solvents Controlled by Polarity. *Angew. Chem., Int. Ed.* **2013**, *52*, 12439−12442.
(48) Zheng, Y.-Z.; Wang, N.-N.; Luo, J.-J.; Zhou, Y.; Yu, Z.-W. Hydrogen-Bonding Interactions between [BMIM][BF_4] and Acetonitrile. *Phys. Chem. Chem. Phys.* **2013**, *15*, 18055−18064.
(49) Ekka, D.; Roy, M. N. Quantitative and Qualitative Analysis of Ionic Solvation of Individual Ions of Imidazolium Based Ionic Liquids in Significant Solution Systems by Conductance and FT-IR Spectroscopy. *RSC Adv.* **2014**, *4*, 19831−19845.
(50) Marekha, B. A.; Kalugin, O. N.; Bria, M.; Takamuku, T.; Gadžurić, S.; Idrissi, A. Competition between Cation-Solvent and Cation-Anion Interactions in Imidazolium Ionic Liquids with Polar Aprotic Solvents. *ChemPhysChem* **2017**, *18*, 718−721.
(51) McDaniel, J. G.; Son, C. Y. Ion Correlation and Collective Dynamics in BMIM/BF_4-Based Organic Electrolytes: From Dilute Solutions to the Ionic Liquid Limit. *J. Phys. Chem. B* **2018**, *122*, 7154−7169.
(52) Marekha, B. A.; Kalugin, O. N.; Bria, M.; Idrissi, A. Probing Structural Patterns of Ion Association and Solvation in Mixtures of Imidazolium Ionic Liquids with Acetonitrile by Means of Relative ^1H and ^{13}C NMR Chemical Shifts. *Phys. Chem. Chem. Phys.* **2015**, *17*, 23183−23194.
(53) Avent, A. G.; Chaloner, P. A.; Day, M. P.; Seddon, K. R.; Welton, T. Evidence for Hydrogen Bonding in Solutions of 1-Ethyl-3-methylimidazolium Halides, and its Implications for Room-temperature Halogenoaluminate(III) Ionic Liquids. *J. Chem. Soc., Dalton Trans.* **1994**, *0*, 3405−3413.
(54) Consorti, C. S.; Suarez, P. A. Z.; de Souza, R. F.; Burrow, R. A.; Farrar, D. H.; Lough, A. J.; Loh, W.; da Silva, L. H. M.; Dupont, J. Identification of 1,3-Dialkylimidazolium Salt Supramolecular Aggregates in Solution. *J. Phys. Chem. B* **2005**, *109*, 4341−4349.
(55) Cade, E. A.; Petenuci, J., III; Hoffmann, M. M. Aggregation Behavior of Several Ionic Liquids in Molecular Solvents of Low Polarity-Indication of a Bimodal Distribution. *ChemPhysChem* **2016**, *17*, 520−529.

https://dx.doi.org/10.1021/acs.jpcb.0c07450
J. Phys. Chem. B 2020, 124, 10776−10786

(56) Hunger, J.; Stoppa, A.; Buchner, R.; Hefter, G. From Ionic Liquid to Electrolyte Solution: Dynamics of 1-N-Butyl-3-N-methylimidazolium Tetrafluoroborate/Dichloromethane Mixtures. *J. Phys. Chem. B* **2008**, *112*, 12913−12919.
(57) Nama, D.; Anil Kumar, P. G.; Pregosin, P. S.; Geldbach, T. J.; Dyson, P. J. ^{1}H, ^{19}F-HOESY and PGSE Diffusion Studies on Ionic Liquids: The Effect of Co-Solvent on Structure. *Inorg. Chim. Acta* **2006**, *359*, 1907−1911.
(58) Cha, S.; Lee, M.; Kim, D. Concentration Dependence of Ion Pairing in Imidazolium-Based Ionic Liquid Solutions. *ChemPhysChem* **2019**, *20*, 482−488.
(59) Sung, W.; Kim, D. Observation of Isolated Ionic Liquid Cations and Water Molecules in an Inert Solvent. *Phys. Chem. Chem. Phys.* **2016**, *18*, 27529−27535.
(60) Mocci, F.; Laaksonen, A.; Wang, J.-L.; Saba, G.; Lai, A.; Marincola, F. C. *The Structure of Ionic Liquids*; Caminiti, R.; Gontrani, L., Eds.; Springer: 2014; Chapter 4, pp 97−126.
(61) Damodaran, K. *Annual Reports on NMR Spectroscopy*; Elsevier Ltd., 2016; pp 215−244.
(62) Weingärtner, H. NMR Studies of Ionic Liquids: Structure and Dynamics. *Curr. Opin. Colloid Interface Sci.* **2013**, *18*, 183−189.
(63) Fannin, A. A., Jr.; King, L. A.; Levisky, J. A.; Wilkes, J. S. Properties of 1,3-Dialkylimidazolium Chloride-Aluminum Chloride Ionic Liquids. 1. Ion Interactions by Nuclear Magnetic Resonance Spectroscopy. *J. Phys. Chem. A* **1984**, *88*, 2609−2614.
(64) Katsyuba, S. A.; Griaznova, T. P.; Vidiš, A.; Dyson, P. J. Structural Studies of the Ionic Liquid 1-Ethyl-3-methylimidazolium Tetrafluoroborate in Dichloromethane Using a Combined DFT-NMR Spectroscopic Approach. *J. Phys. Chem. B* **2009**, *113*, 5046−5051.
(65) Tsuzuki, S.; Tokuda, H.; Mikami, M. Theoretical Analysis of the Hydrogen Bond of Imidazolium C_2-H with Anions. *Phys. Chem. Chem. Phys.* **2007**, *9*, 4780−4784.
(66) Balevicius, V.; Gdaniec, Z.; Aidas, K.; Tamuliene, J. NMR and Quantum Chemistry Study of Mesoscopic Effects in Ionic Liquids. *J. Phys. Chem. A* **2010**, *114*, 5365−5371.
(67) Olsen, J. M. H.; Kongsted, J. Molecular Properties through Polarizable Embedding. *Adv. Quantum Chem.* **2011**, *61*, 107−143.
(68) Nielsen, C. B.; Christiansen, O.; Mikkelsen, K. V.; Kongsted, J. Density Functional Self-Consistent Quantum Mechanics/Molecular Mechanics Theory for Linear and nonlinear Molecular Properties: Applications to Solvated Water and Formaldehyde. *J. Chem. Phys.* **2007**, *126*, No. 154112.
(69) Aidas, K.; Møgelhøj, A.; Nielsen, C. B.; Mikkelsen, K. V.; Ruud, K.; Christiansen, O.; Kongsted, J. Solvent Effects on NMR Isotropic Shielding Constants. A Comparison between Explicit Polarizable Discrete and Continuum Approaches. *J. Phys. Chem. A* **2007**, *111*, 4199−4210.
(70) Aidas, K.; Mikkelsen, K. V.; Kongsted, J. On the Existence of the H3 Tautomer of Adenine in Aqueous Solution. Rationalizations based on Hybrid Quantum Mechanics/Molecular Mechanics Predictions. *Phys. Chem. Chem. Phys.* **2010**, *12*, 761−768.
(71) Eriksen, J. J.; Olsen, J. M. H.; Aidas, K.; Ågren, H.; Mikkelsen, K. V.; Kongsted, J. Computational Protocols for Prediction of Solute NMR Relative Chemical Shifts. A Case Study of L-Tryptophan in Aqueous Solution. *J. Comput. Chem.* **2011**, *32*, 2853−2864.
(72) Kongsted, J.; Aidas, K.; Mikkelsen, K. V.; Sauer, S. P. A. On the Accuracy of Density Functional Theory to Predict Shifts in Nuclear Magnetic Resonance Shielding Constants due to Hydrogen Bonding. *J. Chem. Theory Comput.* **2008**, *4*, 267−277.
(73) Møgelhøj, A.; Aidas, K.; Mikkelsen, K. V.; Sauer, S. P. A.; Kongsted, J. Prediction of Spin-Spin Coupling Constants in Solution based on Combined Density Functional Theory/Molecular Mechanics. *J. Chem. Phys.* **2009**, *130*, No. 134508.
(74) Møgelhøj, A.; Aidas, K.; Mikkelsen, K. V.; Kongsted, J. Solvent Effects on the Nitrogen NMR Shielding and Nuclear Quadrupole Coupling Constants in 1-methyltriazoles. *Chem. Phys. Lett.* **2008**, *460*, 129−136.
(75) Murugan, N. A.; Aidas, K.; Kongsted, J.; Rinkevicius, Z.; Ågren, H. NMR Spin-Spin Coupling Constants in Polymethine Dyes as Polarity Indicators. *Chem. - Eur. J.* **2012**, *18*, 11677−11684.
(76) Lengvinaitė, D.; Aidas, K.; Kimtys, L. Molecular Aggregation in Liquid Acetic Acid: Insight from Molecular Dynamics/Quantum Mechanics Modelling of Structural and NMR Properties. *Phys. Chem. Chem. Phys.* **2019**, *21*, 14811−14820.
(77) Bagno, A.; D'Amico, F.; Saielli, G. Computing the NMR Spectrum of a Bulk Ionic Liquid Phase by QM/MM Methods. *J. Phys. Chem. B* **2006**, *110*, 23004−23006.
(78) Bagno, A.; D'Amico, F.; Saielli, G. Computing the ^{1}H NMR Spectrum of a Bulk Ionic Liquid from Snapshots of Car-Parrinello Molecular Dynamics Simulations. *ChemPhysChem* **2007**, *8*, 873−881.
(79) Case, D. A.; Darden, T. A.; Cheatham, T. E., III; Simmerling, C. L.; Wang, J.; Duke, R. E.; Luo, R.; Walker, R. C.; Zhang, W.; Merz, K. M. et al. *Amber12*; University of California: San Francisco, 2012.
(80) Hehre, W. J.; Ditchfield, R. J.; Pople, J. A. Self-Consistent Molecular Orbital Methods. XII. Further Extensions of Gaussian-Type Basis Sets for Use in Molecular Orbital Studies of Organic Molecules. *J. Chem. Phys.* **1972**, *56*, 2257−2261.
(81) Hariharan, P. C.; Pople, J. A. The Influence of Polarization Functions on Molecular Orbital Hydrogenation Energies. *Theor. Chim. Acta* **1973**, *28*, 213−222.
(82) Frisch, M. J.; Trucks, G. W.; Schlegel, H. B.; Scuseria, G. E.; Robb, M. A.; Cheeseman, J. R.; Scalmani, G.; Barone, V.; Mennucci, B.; Petersson, G. A. et al. *Gaussian 09*, revision D.01; Gaussian, Inc.: Wallingford, CT, 2010.
(83) Liu, Z.; Huang, S.; Wang, W. A Refined Force Field for Molecular Simulation of Imidazolium-Based Ionic Liquids. *J. Phys. Chem. B* **2004**, *108*, 12978−12989.
(84) Cornell, W. D.; Cieplak, P.; Bayly, C. I.; Gould, I. R.; Merz, K. M.; Ferguson, D. M.; Spellmeyer, D. C.; Fox, T.; Caldwell, J. W.; Kollman, P. A. A Second Generation Force Field for the Simulation of Proteins, Nucleic Acids, and Organic Molecules. *J. Am. Chem. Soc.* **1995**, *117*, 5179−5197.
(85) Wang, J.; Wolf, R. M.; Caldwell, J. W.; Kollman, P. A.; Case, D. A. Development and of a General Amber Force Field of a General Amber Force Field. *J. Comput. Chem.* **2004**, *25*, 1157−1174.
(86) Bayly, C. I.; Cieplak, P.; Cornell, W.; Kollman, P. A. A Well-Behaved Electrostatic Potential based Method using Charge Restraints for Deriving Atomic Charges: the RESP Model. *J. Phys. Chem. A* **1993**, *97*, 10269−10280.
(87) Wang, J.; Wang, W.; Kollman, P. A.; Case, D. A. Automatic Atom Type and Bond Type Perception in Molecular Mechanical Calculations. *J. Mol. Graphics Modell.* **2006**, *25*, 247−260.
(88) Jorgensen, W. L. Quantum and Statistical Mechanical Studies of Liquids. 10. Transferable Intermolecular Potential Functions for Water, Alcohols, and Ethers. Application to Liquid Water. *J. Am. Chem. Soc.* **1981**, *103*, 335−340.
(89) Martínez, L.; Andrade, R.; Birgin, E. G.; Martínez, J. M. Packmol: A package for Building Initial Configurations for Molecular Dynamics Simulations. *J. Comput. Chem.* **2009**, *30*, 2157−2164.
(90) Ryckaert, J.-P.; Ciccotti, G.; Berendsen, H. J. C. Numerical Integration of the Cartesian Equations of Motion of a System with Constraints: Molecular Dynamics of n-Alkanes. *J. Comput. Phys.* **1977**, *23*, 327−341.
(91) Miyamoto, S.; Kollman, P. A. Settle: An Analytical Version of the SHAKE and RATTLE Algorithm for Rigid Water Models. *J. Comput. Chem.* **1992**, *13*, 952−962.
(92) Becke, A. D. Density-Functional Thermochemistry. III. The Role of Exact Exchange. *J. Chem. Phys.* **1993**, *98*, 5648−5652.
(93) Kendall, R. A.; Dunning, T. H.; Harrison, R. J. Electron Affinities of the First−Row Atoms Revisited. Systematic Basis Sets and Wave Functions. *J. Chem. Phys.* **1992**, *96*, 6796−6806.
(94) Dunning, T. H. Gaussian Basis Sets for Use in Correlated Molecular Calculations. I. The Atoms Boron through Neon and Hydrogen. *J. Chem. Phys.* **1989**, *90*, 1007−1023.

https://dx.doi.org/10.1021/acs.jpcb.0c07450
J. Phys. Chem. B 2020, 124, 10776−10786

(95) Adamo, C.; Barone, V. Toward Reliable Density Functional Methods without Adjustable Parameters: The PBE0 Model. *J. Chem. Phys.* **1999**, *110*, 6158−6170.
(96) Keal, T. W.; Tozer, D. J. A Semiempirical Generalized Gradient Approximation Exchange-Correlation Functional. *J. Chem. Phys.* **2004**, *121*, 5654−5660.
(97) Weigend, F.; Ahlrichs, R. Balanced Basis Sets of Split Valence, Triple Zeta Valence and Quadruple Zeta Valence Quality for H to Rn: Design and Assessment of Accuracy. *Phys. Chem. Chem. Phys.* **2005**, *7*, 3297−3305.
(98) Woon, D. E.; Dunning, T. H., Jr. Gaussian Basis Sets for Use in Correlated Molecular Calculations. V. Core−Valence Basis Sets for Boron through Neon. *J. Chem. Phys.* **1995**, *103*, 4572−4585.
(99) Aidas, K.; Angeli, C.; Bak, K. L.; Bakken, V.; Bast, R.; Boman, L.; Christiansen, O.; Cimiraglia, R.; Coriani, S.; Dahle, P.; et al. The Dalton Quantum Chemistry Program System. *WIREs Comput. Mol. Sci.* **2014**, *4*, 269−284.
(100) Matthews, D. A.; Cheng, L.; Harding, M. E.; Lipparini, F.; Stopkowicz, S.; Jagau, T.-C.; Szalay, P. G.; Gauss, J.; Stanton, J. F. Coupled-Cluster Techniques for Computational Chemistry: The CFOUR Program Package. *J. Chem. Phys.* **2020**, *152*, No. 214108.
(101) Kongsted, J.; Nielsen, C. B.; Mikkelsen, K. V.; Christiansen, O.; Ruud, K. Nuclear Magnetic Shielding Constants of Liquid Water: Insights from Hybrid Quantum Mechanics/Molecular Mechanics Models. *J. Chem. Phys.* **2007**, *126*, No. 034510.
(102) Tomasi, J.; Mennucci, B.; Cammi, R. Quantum Mechanical Continuum Solvation Models. *Chem. Rev.* **2005**, *105*, 2999−3093.
(103) Breneman, C. M.; Wiberg, K. B. Determining Atom-Centered Monopoles from Molecular Electrostatic Potentials. The need for High Sampling Density in Formamide Conformational Analysis. *J. Comput. Chem.* **1990**, *11*, 361−373.
(104) Ahlström, P.; Wallqvist, A.; Engström, S.; Jönsson, B. A Molecular Dynamics Study of Polarizable Water. *Mol. Phys.* **1989**, *68*, 563−581.
(105) Chen, S.; Vijayaraghavan, R.; MacFarlane, D. R.; Izgorodina, E. I. Ab Initio Prediction of Proton NMR Chemical Shifts in Imidazolium Ionic Liquids. *J. Phys. Chem. B* **2013**, *117*, 3186−3197.
(106) Hunt, P. A.; Gould, I. R. Structural Characterization of the 1-Butyl-3-methylimidazolium Chloride Ion Pair Using ab Initio Methods. *J. Phys. Chem. A* **2006**, *110*, 2269−2282.
(107) Hunt, P. A.; Kirchner, B.; Welton, T. Characterising the Electronic Structure of Ionic Liquids: An Examination of the 1-Butyl-3-Methylimidazolium Chloride Ion Pair. *Chem. - Eur. J.* **2006**, *12*, 6762−6775.
(108) Spickermann, C.; Thar, J.; Lehmann, B. C.; Zahn, S.; Hunger, J.; Buchner, R.; Hunt, P. A.; Welton, T.; Kirchner, B. Computational Protocols for Prediction of Solute NMR Relative Chemical Shifts. A Case Study of L-Tryptophan in Aqueous Solution. *J. Chem. Phys.* **2008**, *129*, No. 104505.
(109) Marekha, B. A.; Koverga, V. A.; Chesneau, E.; Kalugin, O. N.; Takamuku, T.; Jedlovszky, P.; Idrissi, A. Local Structure in Terms of Nearest-Neighbor Approach in 1-Butyl-3-methylimidazolium-Based Ionic Liquids: MD Simulations. *J. Phys. Chem. B* **2016**, *120*, 5029−5041.
(110) Hardacre, C.; Holbrey, J. D.; McMath, S. E. J.; Bowron, D. T.; Soper, A. K. Structure of Molten 1,3-Dimethylimidazolium Chloride using Neutron Diffraction. *J. Chem. Phys.* **2003**, *118*, 273−278.
(111) Palomar, J.; Ferro, V. R.; Gilarranz, M. A.; Rodriguez, J. J. Computational Approach to Nuclear Magnetic Resonance in 1-Alkyl-3-methylimidazolium Ionic Liquids. *J. Phys. Chem. B* **2007**, *111*, 168−180.

https://dx.doi.org/10.1021/acs.jpcb.0c07450
J. Phys. Chem. B 2020, 124, 10776−10786